27-737 Data Analytics for Materials Science

Powder Classification

Srujana Yarasi, Andrew Kitahara, Ryan Cohn, Elizabeth Holm, Anthony Rollett

Materials Sci. & Eng., Carnegie Mellon University, Pittsburgh, PA.

Revised:
Apr. 28th, 2021

Introduction

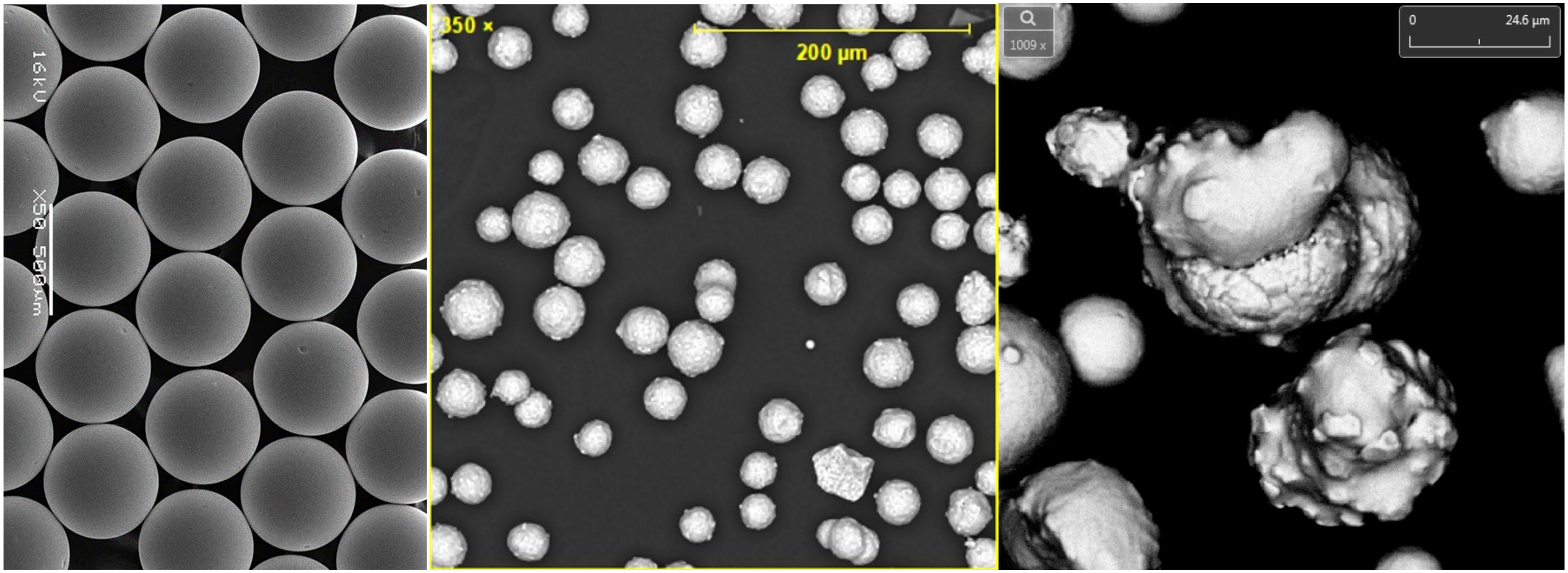

There are different kinds of powders, ranging from perfectly spherical (made with highly expensive processes such as PREP) to highly crunchy (with irregular surface morphology) and then those in between. And these differences in powder characteristics matter a lot! Why?

Carnegie Mellon University

Part I : Powder Flow in Metal Powder Bed AM

Why measure powder flow?

Two modes of powder flow occur in electron beam powder bed AM machines
- Flow from hopper (vertical)
- Build plate spreading (horizontal)

Powder flow is important because it affects layer generation capabilities which include powder layer density, thickness, laser absorption, and thermal conductivity.

Understanding powder flow is important for process parameter tuning.
And to understand powder flow, we must understand the particle characteristics that affect it.

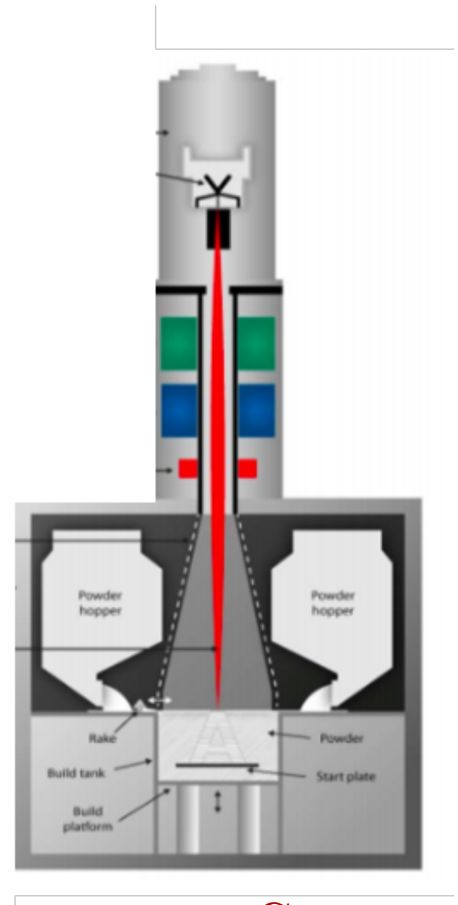

Carnegie Mellon University

Powder Flow in Metal Powder Bed AM

Assuming spherical particles is unrealistic leading to incorrect flow characterization.

Particle size distribution (PSD) is the standard way to measure powders but excludes surface texture, morphology, and defects.

This results in porosity and other types of build defects that can lead to mechanical failure.

To avoid incorrect flow characterization and these types of defects, we need to better understand the physical characteristics of powder like surface morphology, shape, agglomerates.

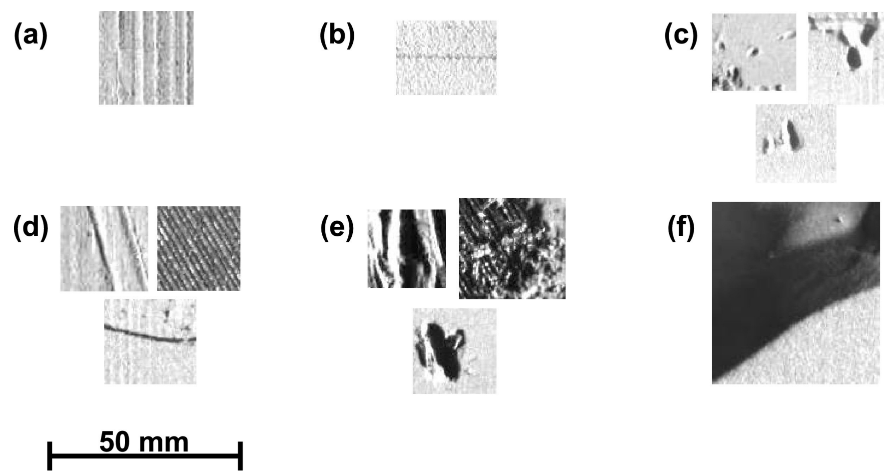

Representative examples of the six different powder bed anomaly classes (a) Recoater hopping, (b) Recoater streaking, (c) Debris, (d), Super-elevation, (e) Part failure, and (f) Incomplete spreading.
Scime, Luke *et al Additive Manufacturing* 19 (2018): 114-126

Flowability

Characteristics of the powder feedstock such as particle size distribution, sphericity, powder porosity, surface texture, and internal defects affect powder flow and performance.

To improve powder bed processes, it is important to characterize and categorize these aspects of powder feedstock efficiently.

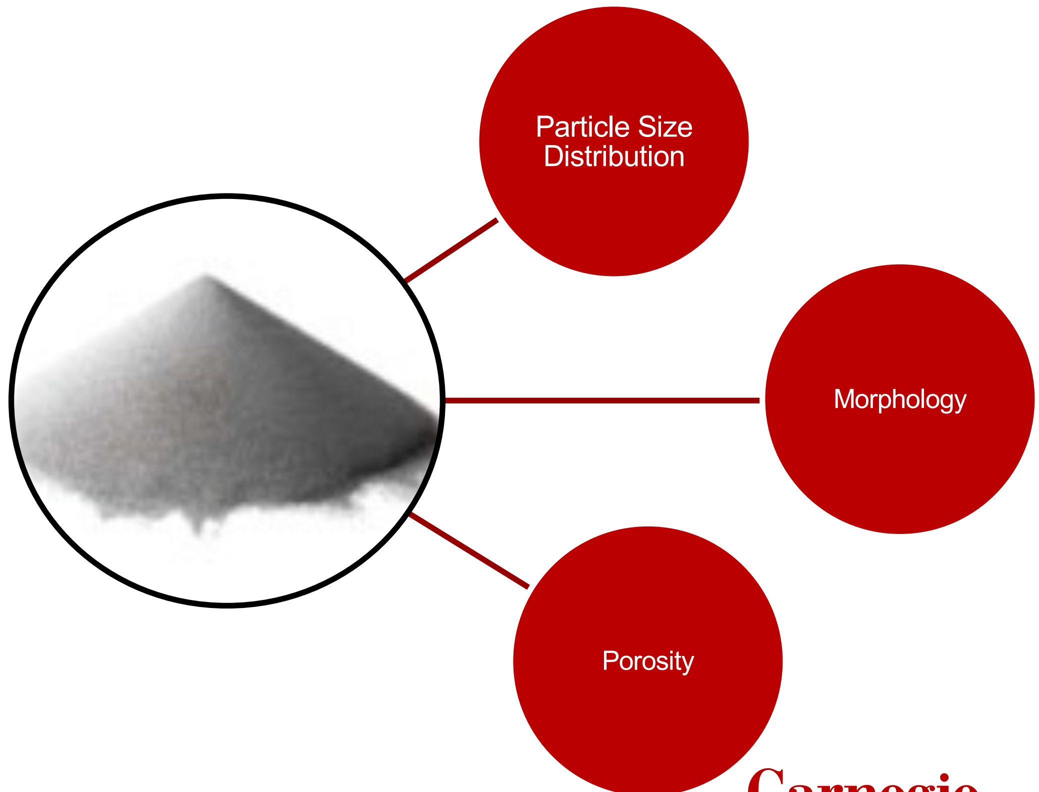

Carnegie Mellon University

Measuring Flowability

- Hall Flowmeter- This is a fairly simple instrument but is ineffective in accurately representing powder flow in an AM machine.
- FT4 Rheometer- It better represents powder flow through parameters, like BFE and SE, that mimic powder flow across the build plate and through the hopper.
- Granudrum- The dynamic measurement of the angle of repose is linked to cohesion, which is an important factor that determined spreadability.

Carnegie Mellon University

Methods: Flow Properties from Rheometer

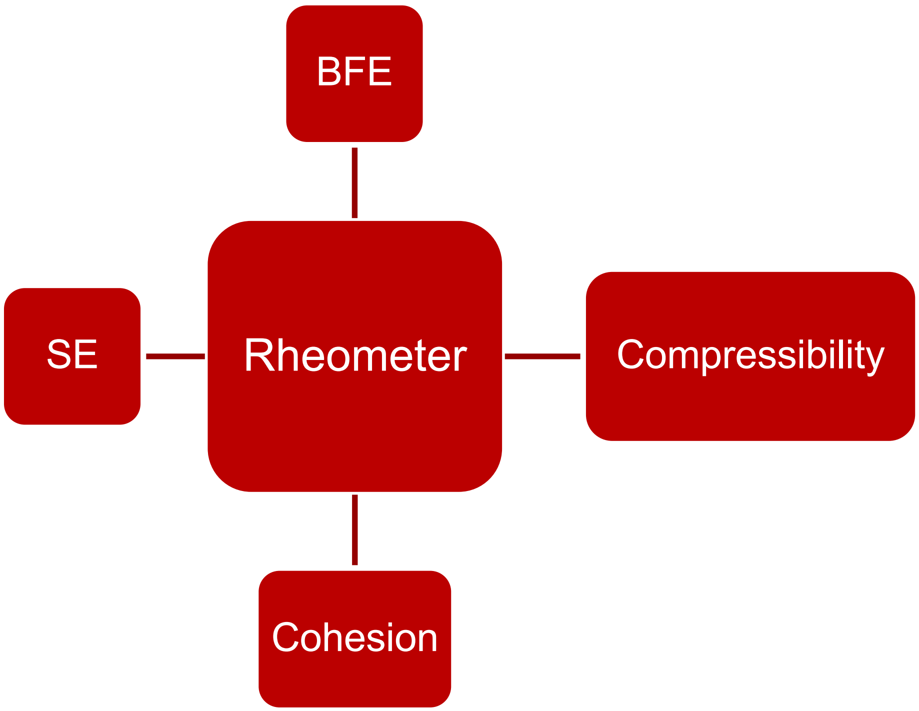

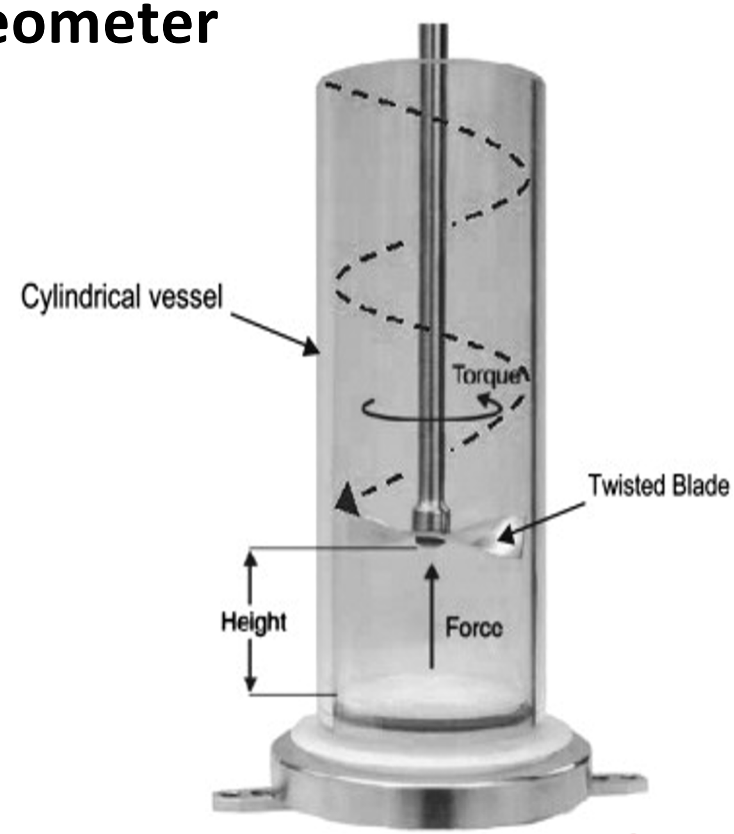

Freeman FT4 Rheometer Apparatus

Methods: Flow Properties from Rheometer

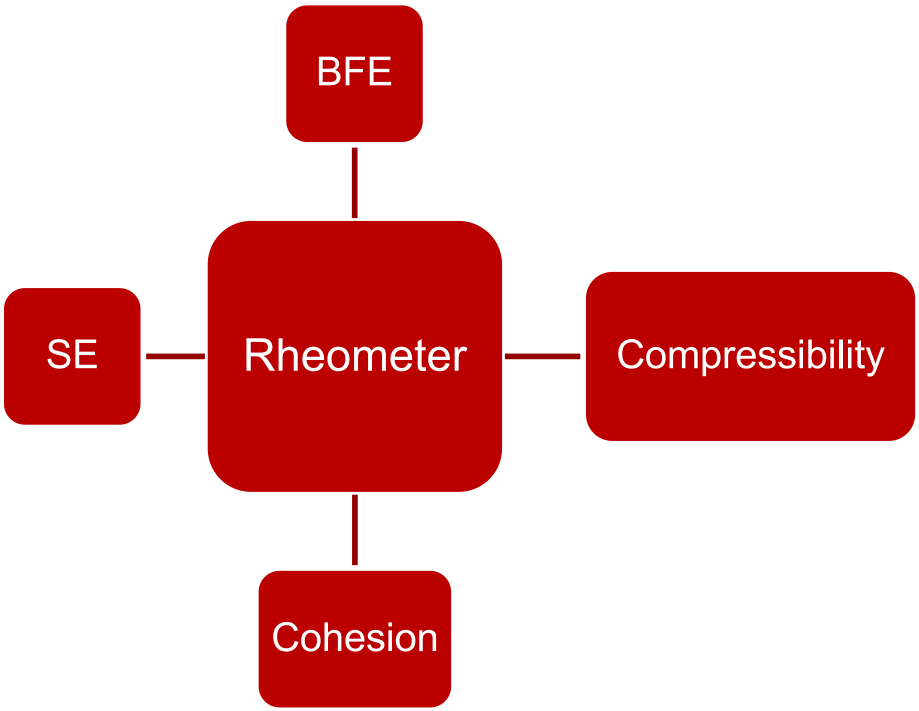

- BFE: Basic Flowability Energy is the measure of the powder's flowability in forced flow conditions.
- SE: Specific Energy is the measure of the powder's flowability in unconfined flow conditions.
- Compressibility is an indirect measure of flowability relating to process environments, such as storage in hoppers or behavior during roller compaction.
- Cohesion is measured from shear tests.

Carnegie Mellon University

Part II : Powder Characteristics

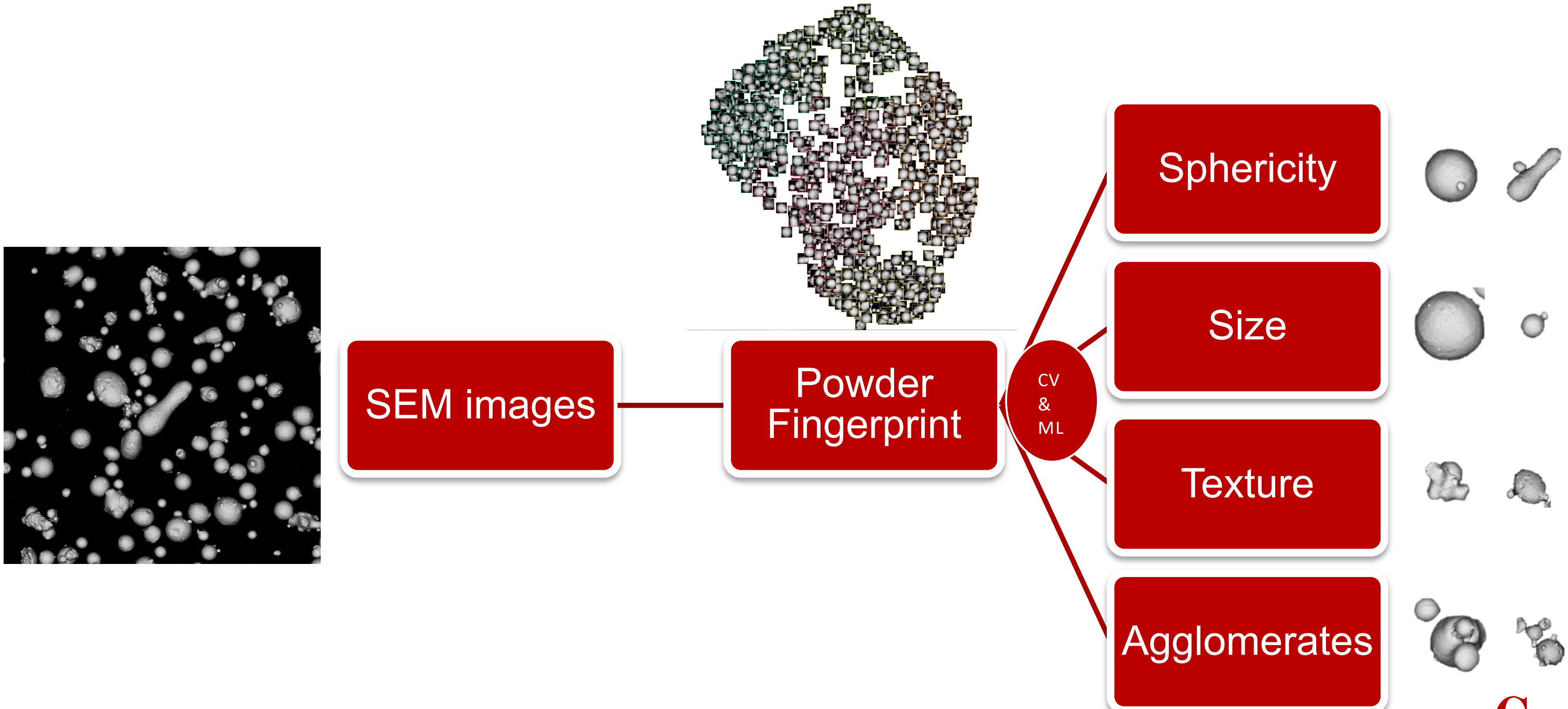

Carnegie Mellon University

Image Pre-Processing and Particle Labeling

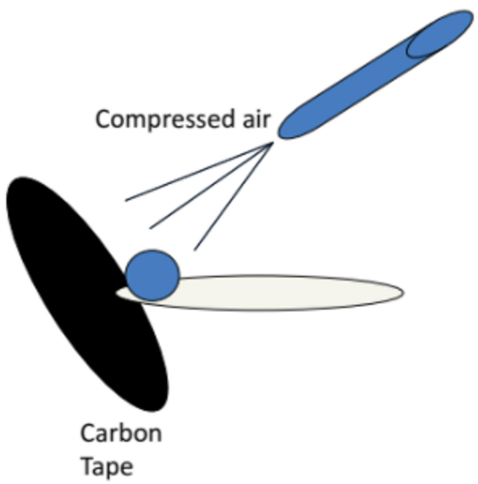

SEM Prep

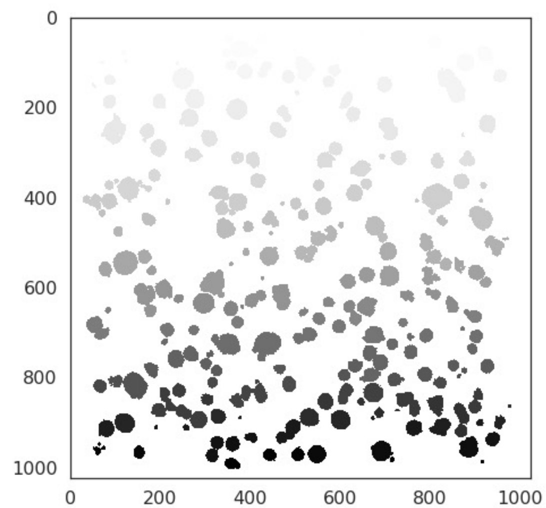

Thresholded image of Steel Powder

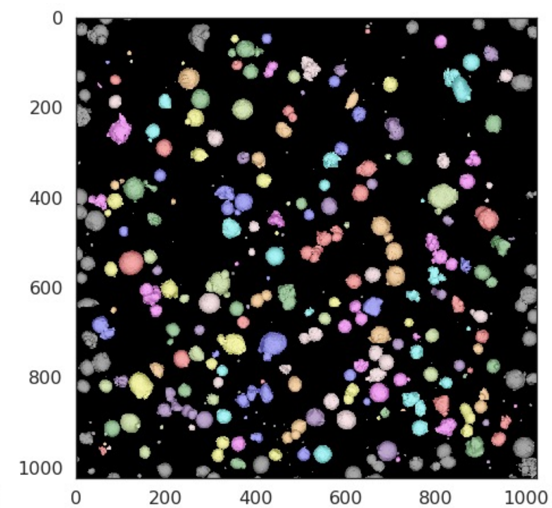

Particles are segmented and labeled

SEM Imaging → Thresholding → Particle Segmentation → Particle Labeling

Carnegie Mellon University

A Previous Project on Computer Vision for Powder Classification

The following series of slides describes a project from the 2014-2016 period to use computer vision methods to classify powders. This was a successful effort but note that a fixed set of image filters was used such as Harris corners. This was largely the work of Brian DeCost in Prof. Holm's group. This approach has been supplanted (for the most part) by Convolutional Neural Nets which automate the process of determining which filters are most effective for a given task.

Use of non-Standard Powders in LPBF

"A Database Relating Powder Properties to Process Outcomes for Direct Metal AM"

America Makes supported project 2014-2016

Geometries: NIST part with 8 Cylinders Surrounding it

Goal: Increase the range of powders useable in Arcam and EOS machines

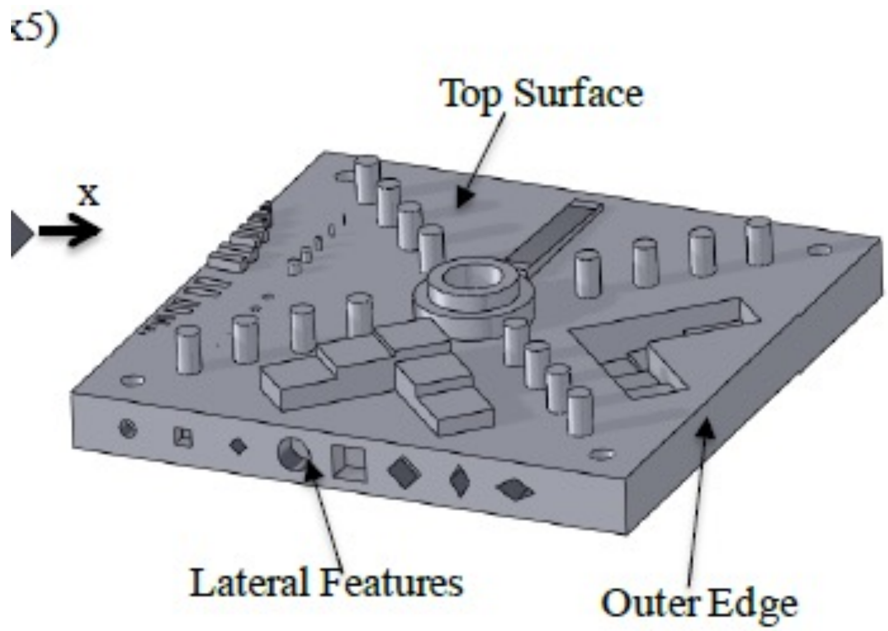

Carnegie Mellon University

7 Powder Systems

- 7 powder systems (PS) + 1 Arcam Ti64 + 1 EOS Ti64 powders as control.
- 3 PS used for Arcam EBM and 4 PS for EOS DMLS.
- 3 different powder production processes: Gas Atomization, PREP, HDH+PS
- A wide range of particle size distributions for 7 PS.

Powder System	Material	Machine used in	Mesh size	Powder size (µm)	Powder production
#0 Arcam Control	Ti64	Arcam EBM	-140/+325	44-105	Gas atomization
#1		Arcam EBM	-120/+325	44-125	HDH+PS
#2		Arcam EBM	-60/+120	125-250	PREP
#3		EOS DMLS	-170	<88	PREP
#4		EOS DMLS	-200/+325	44-74	HDH+PS
#5		EOS DMLS	-140/+325	44-105 "ArcamEOS Build"	HDH+PS
#6		Arcam EBM	-100/+325	44-149	PREP
#7	IN718	EOS DMLS	-170/+800	15-88	Gas atomization
#8 EOS Control	Ti64	EOS DMLS	-230/+800	15-63	Gas atomization

Standard NIST Part, Eight Different Powders

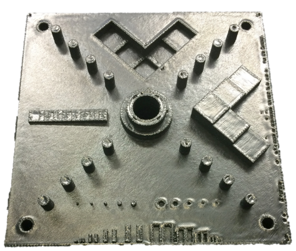

PS 0-70

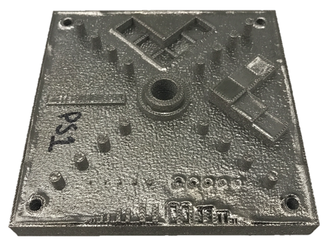

PS 1-70

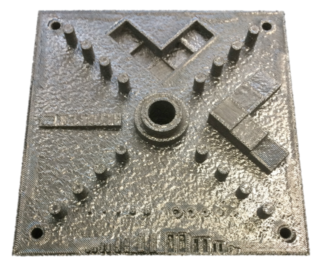

PS 2-100

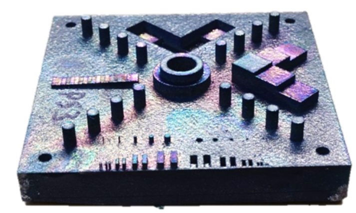

PS 3-60

PS 4-60

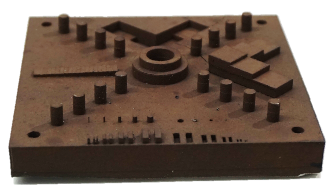

PS 5-60

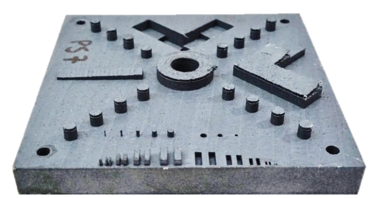

PS 7-60

PS 8-60

Carnegie Mellon University

Powder Characteristics versus Flow Behavior

- Gas-atomized powders generally display a log-normal size distribution[1]
- Log-normal distribution will appear linear on adjusted cumulative probability plot

- Deviation from log-normal suggests sudden change in distribution (sieving)
- AlSi10Mg powder does not deviate from log normal
- EOS Ti-6Al-4V does not follow this trend

[1] O.D. Neikov, Chapter 5 - Atomization and Granulation, In Handbook of Non-Ferrous Metal Powders, edited by Neikov et al., Elsevier, Oxford, 2009, Pages 102-142

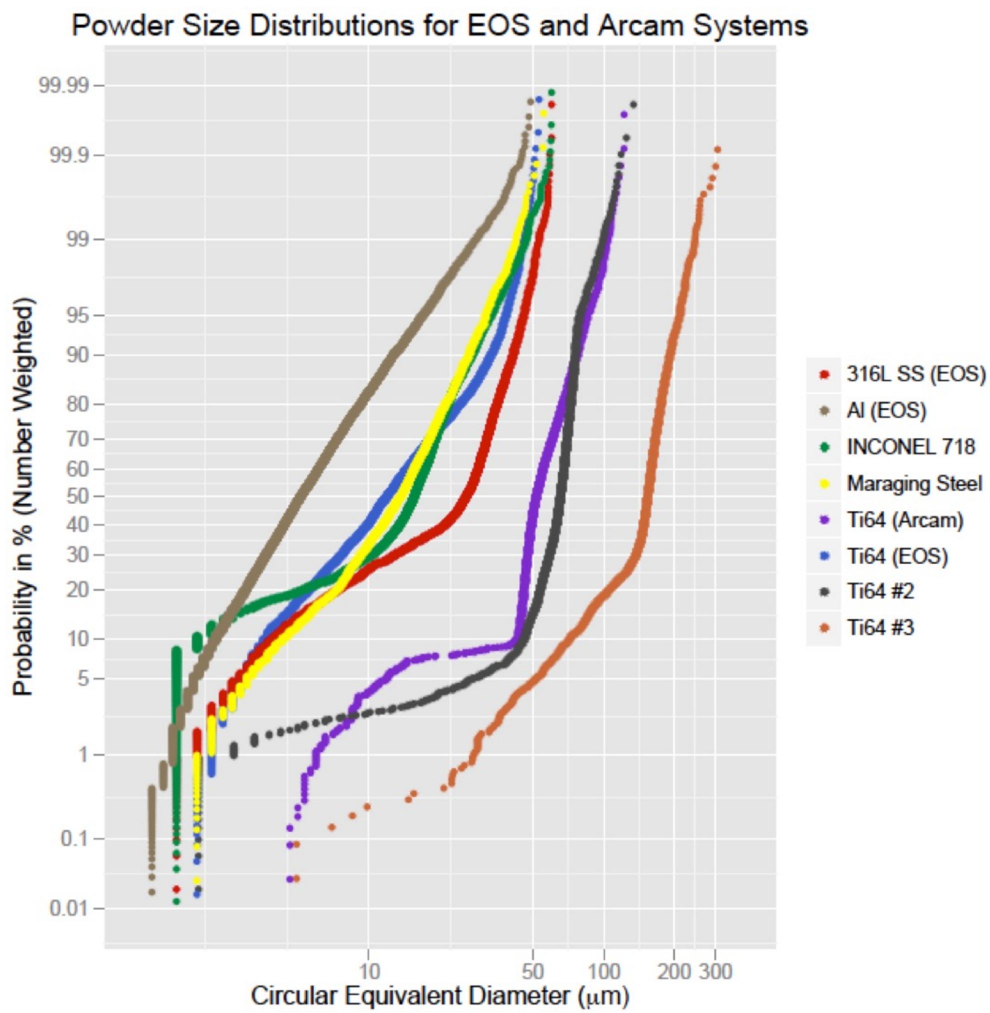

Types of powders to classify

Machine	Material	Manf. Method
Arcam (>50μm)	ARCAM Ti-6Al-4V	Plasma Atomized
	Ti-6Al-4V #2	HDH + PS*
	TI-6Al-4V #3 (Large)	PREP
EOS (<60μm)	EOS Ti-6Al-4V	Gas Atomized
	EOS AlSi10Mg	Gas Atomized
	EOS 316L SS	Gas Atomized
	EOS MS1 Maraging Steel	Gas Atomized
	EOS Inconel 718	Gas Atomized

*Hydride/Dehydride + Plasma Spheroidization

Carnegie Mellon University

Size Distribution

SEM

Threshold

Watershed

Size distribution

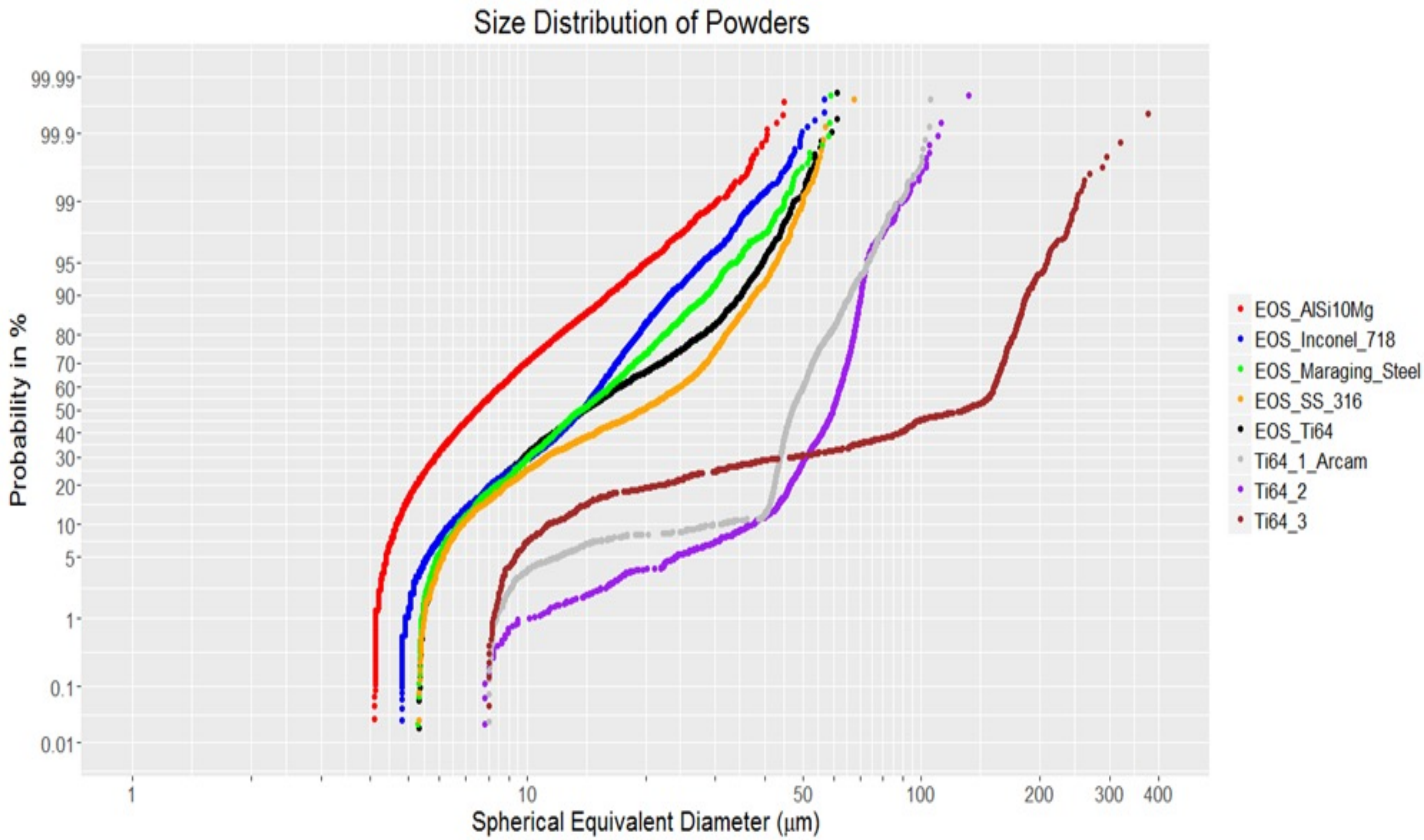

University

Methodology: Step 1: pre-Processing of Images

- 24 images per powder system for training the system from 2 to 4 samples.
- Take SEM micrographs and perform image processing

Adaptive Histogram Equalization

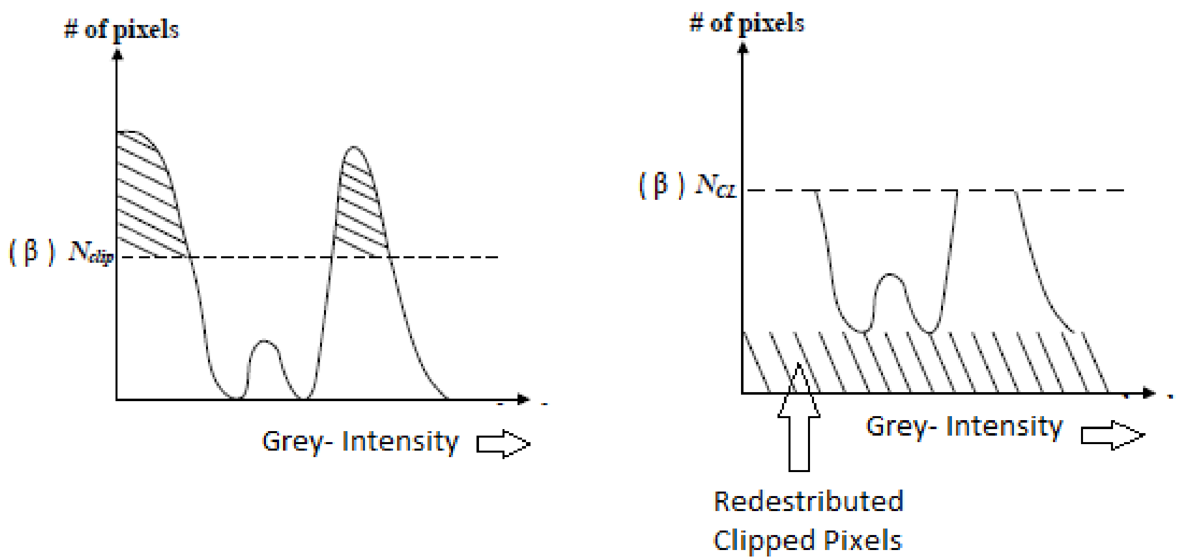

A) Probability Histogram

B) Clipped Histogram

Carnegie Mellon University

Methodology : Step 2 : Computer Vision Pipeline

- Extract Features
- SIFT to find feature descriptor

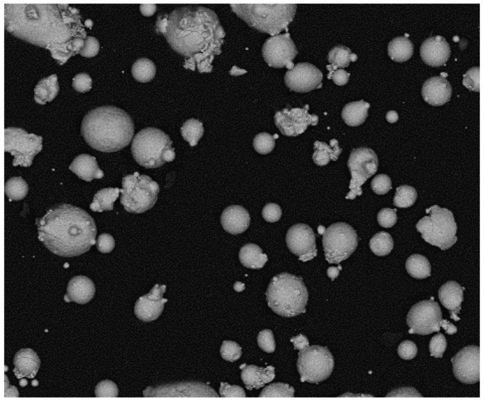

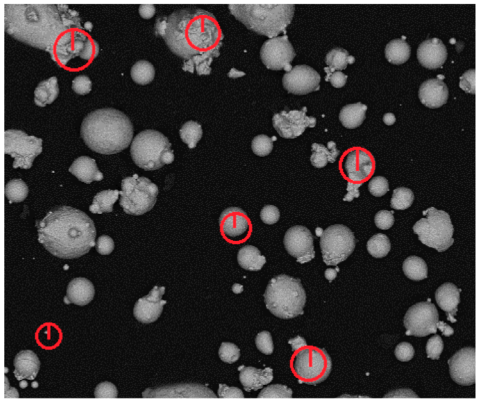

- Clustering to find Visual Words
- Most common features
- Representative of dataset

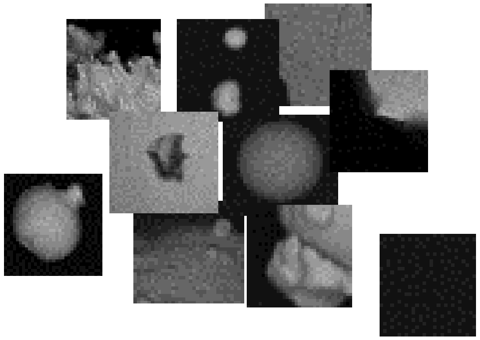

Visual Words

Not Real – Just for illustration

Carnegie Mellon University

Scale-Invariant Feature Transform (SIFT)

Difference of Gaussians:
Lowe, D. G. (1999), 'Object recognition from local scale-invariant features', *ICCV*, 1150-1157.

Harris-LaPlace methods
Mikolajczyk, K. & Schmid, C. (2001), 'Indexing based on scale invariant interest points', *ICCV*, 525-531.

Carnegie Mellon University

Difference of Gaussians

The 1999 paper by Lowe is remarkably simple with only one equation to indicate the numerical calculation of derivatives. The image gradient magnitude M_{ij} and orientation R_{ij} at each point A_{ij} are given by:

$$M_{ij} = \sqrt{(A_{ij} - A_{i+1,j})^2 + (A_{ij} - A_{i,j+1})^2}$$

$$R_{ij} = \mathrm{atan2}\left(A_{ij} - A_{i+1,j}, A_{i,j+1} - A_{ij}\right)$$

The resulting derivative field is examined for maxima and minima where at least one level of nearest neighbor points are checked. Generally, one expects to obtain ≈1,000 points from a 512x512 image.

Example given of the ability of the algorithm to find a similar set of points under rotation and scaling.

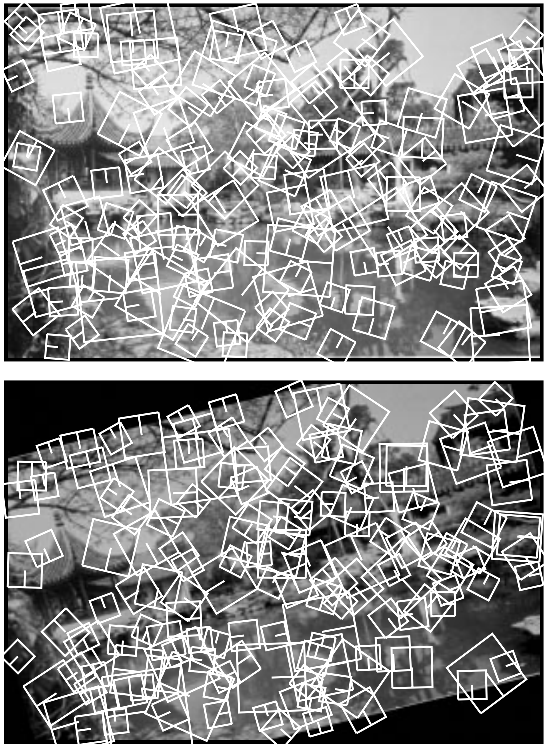

Figure 1: The second image was generated from the first by rotation, scaling, stretching, change of brightness and contrast, and addition of pixel noise. In spite of these changes, 78% of the keys from the first image have a closely matching key in the second image. These examples show only a subset of the keys to reduce clutter.

Harris-LaPlace method

The 2001 paper by Mikolajczyk & Schmid presents an algorithm for *interest point detection* that is invariant to scale changes over a significant range.

Derivatives are computed from the image (intensity) over a range of scales (in a given image). The Harris function is used to identify interest points at each scale but the Laplacian is used to find commonality between points at different scales.

One example from their paper is shown with photos at very different angles of the same apartment block.

A significant advantage of the method is the ability to find features at different magnifications (and orientations) of the same object.

Figure 7: Example of images taken from different view points. There are 14 inliers to a robustly estimated fundamental matrix, all of them are correct. The estimated scale factor is 2.7.

Methodology: Step 2: Computer Vision Pipeline

- Image Representation
- 100 features (Words)
- Feed this to SVM

Image Histogram

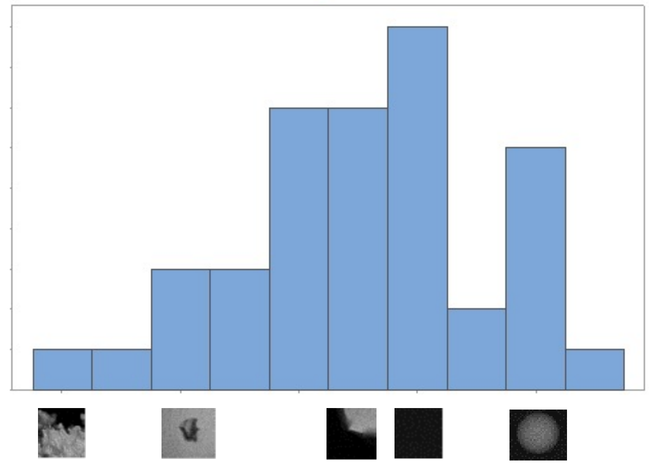

- Use χ2 ("chi-square") distance to compare histograms

$$d(\mathbf{x}_u, \mathbf{x}_v) = \frac{1}{2} \sum_{n=1}^{N} \frac{[x_u(n) - x_v(n)]^2}{x_u(n) + x_v(n)}.$$

- Support Vector Machine (SVM) to classify powders according to powder system

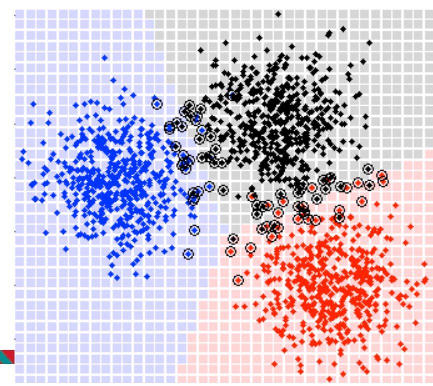

Not Real – Just for illustration

Carnegie Mellon University

Support Vector Machine (SVM)

An SVM is a system for classification.

Originally developed by Vladimir N. Vapnik and Alexey Ya. Chervonenkis in 1963 (1968? See below).

The idea is to find a way to arrange the data such that there is a hyperplane w that separates it into two sets with a gap ("margin") in between. The equation for the hyperplane is $w \cdot x - b = 0$.

Each datapoint is a vector x (of arbitrary dimension). Associated with each vector is a y value which (for 2 classes) is assigned -1 or +1 to indicate to which class it belongs.

V. N. Vapnik and A. Ya. Chervonenkis, "On the uniform convergence of relative frequencies of events to their probabilities," *Proceedings of the USSR Academy of Sciences*, Vol. 181, No. 4 (1968), pp. 781–783. Translated by the American Mathematical Society as *Soviet Mathematics*, Vol. 9 (1968), pp. 915–918.

Support Vector Machine (SVM): 2

The diagram illustrates the maximum-margin hyperplane and margins for an SVM that classifies data into two classes. The *support vectors* are the points (samples) that are situated on the edges (margins).

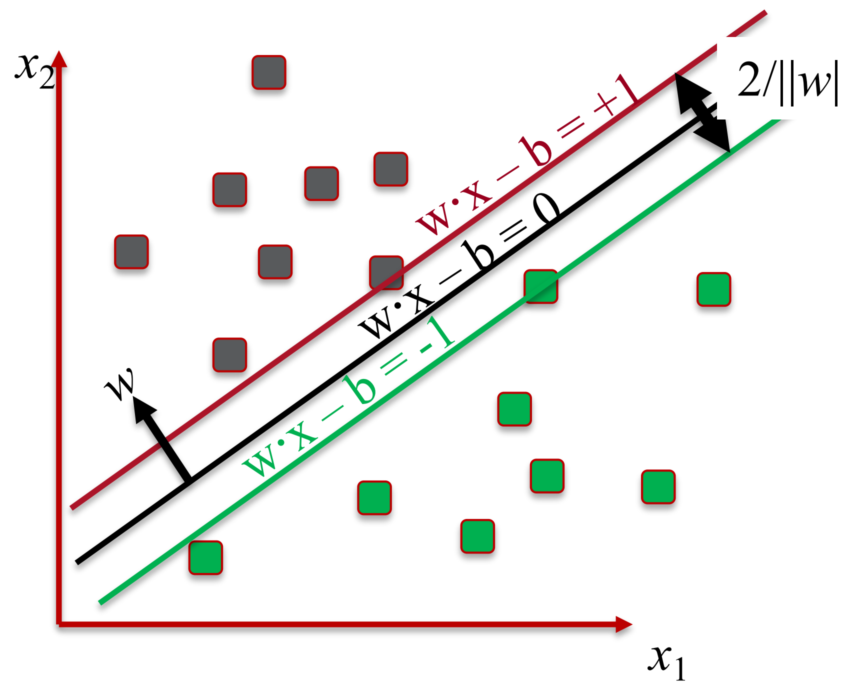

The normal (vector) to the hyperplane is *not*, in general, a unit vector and its magnitude, $||w||$, is related to the size of the margin.

Carnegie Mellon University

Support Vector Machine (SVM): 3

The objective is to separate all the points by finding the hyperplane. Based on the indicator function implied by the values {-1,+1} of the y_i, the desired result is

$$y_{\mathrm{i}}\,(w{\cdot}x_{\mathrm{i}}) - b \geq 1$$

For the fully separable case, it turns out that the margin is determined by the points that lie along the edges of the margin, which is why those points are known as the support vectors.

Of course, few datasets are linearly separable in their entirety so there is a soft margin version with a parameter λ that allows the depth of the margin to be optimized.

$$\left[\frac{1}{n}\sum_{i=1}^{N} max(0, 1 - y_i(w \cdot x_i - b))\right] + \lambda||w||^2$$

Beyond this basic analysis, modern SVM packages use
a variety of procedures to optimize the classification
such as gradient descent, sub-gradient descent, and coordinate descent (to name but a few)).

egie
n
University

ARCAM-size

EOS-size

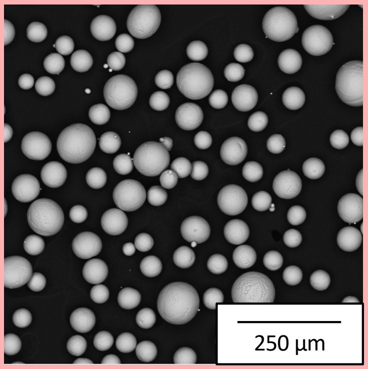

Arcam Ti-6Al-4V

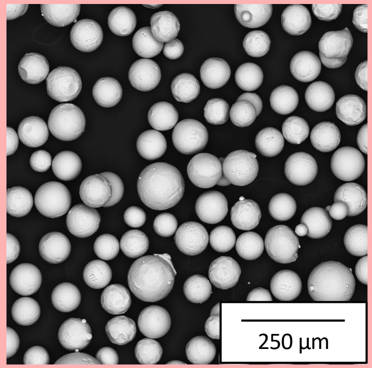

HDH +PS Ti64

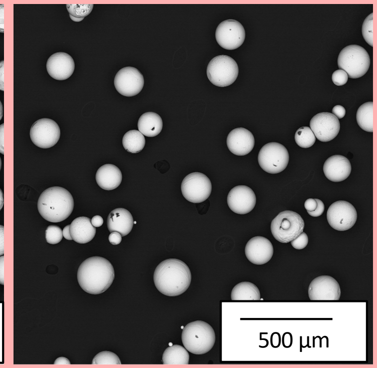

PREP Ti64

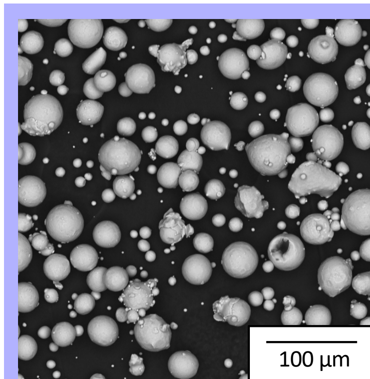

EOS Ti-6Al-4V

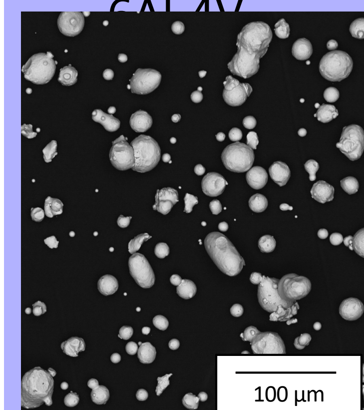

EOS MS1 Maraging Steel

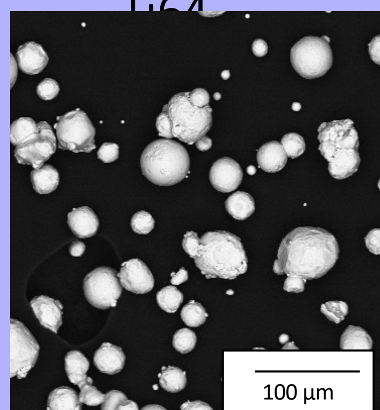

EOS 316L SS

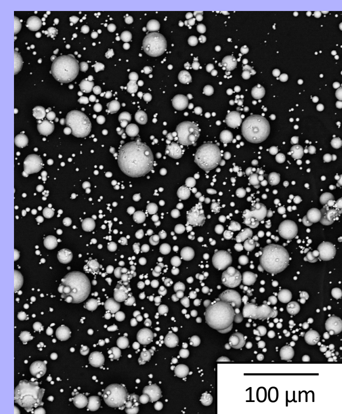

EOS AlSi10Mg

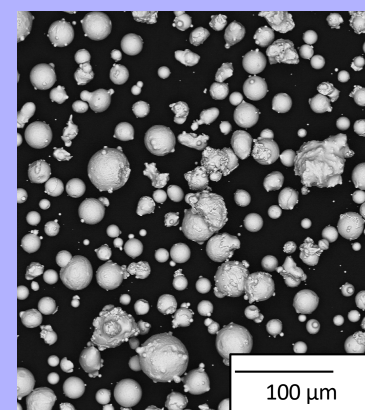

Inconel 718

Computer Vision: SIFT-VLAD

DeCost *et al*. (2017) *JOM* **69** 456

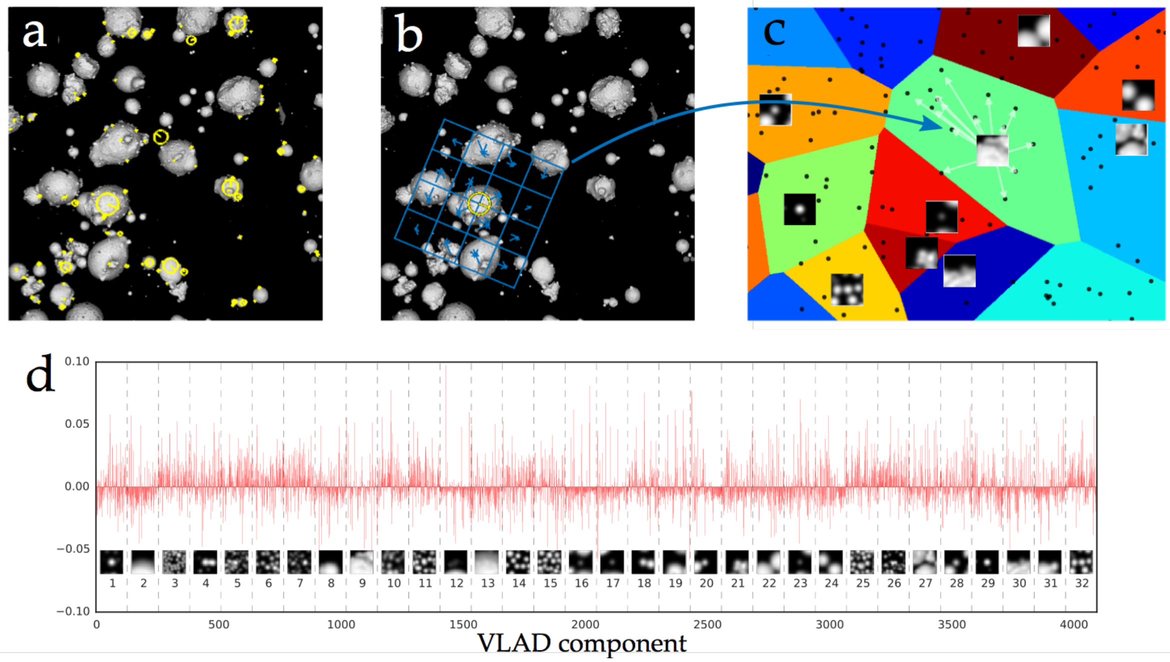

Figure 4. A schematic diagram illustrating the construction of SIFT-VLAD microstructure representations. (a) Select oriented interest points (yellow markers) from a powder micrograph (100 randomly selected interest points shown). (b) Compute a SIFT descriptor (blue grid) for each interest point. (c) Cluster SIFT descriptors (colored regions) such that SIFT descriptors (black dots) are associated with their most similar visual word (image patches); compute a residual vector for each visual word (white arrows). (d) Concatenate the normalized residual vectors (red bars) of each visual word (image patches) to construct the VLAD representation, which serves as a microstructure fingerprint.

SIFT, k-means, VLAD

Scale-invariant feature transform (SIFT) was used to quantify features of interest in the images.

k-means clustering was used to partition 15 % of the SIFT descriptors extracted from the training images into 32 visual words

A vector of locally aggregated descriptors (VLAD) encoding was used to compute the difference between the description of the current image and the center of the corresponding word.

The net result then has a dimension that is the product of the word length and the number of words.

Computer Vision: Confusion Matrices

Cross-validation test set

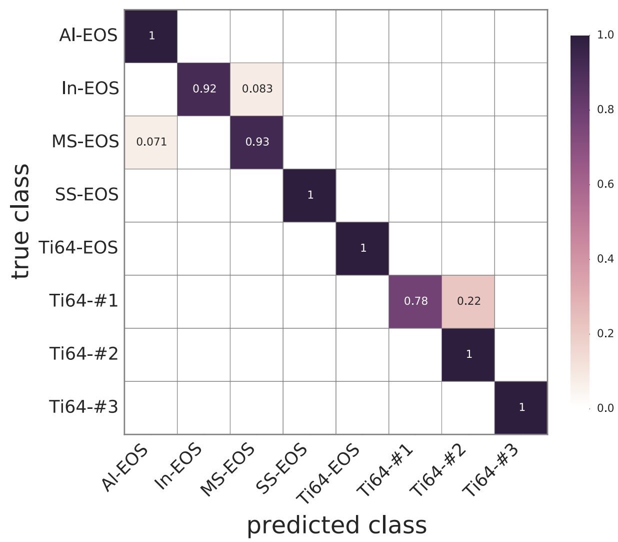

Independent test set

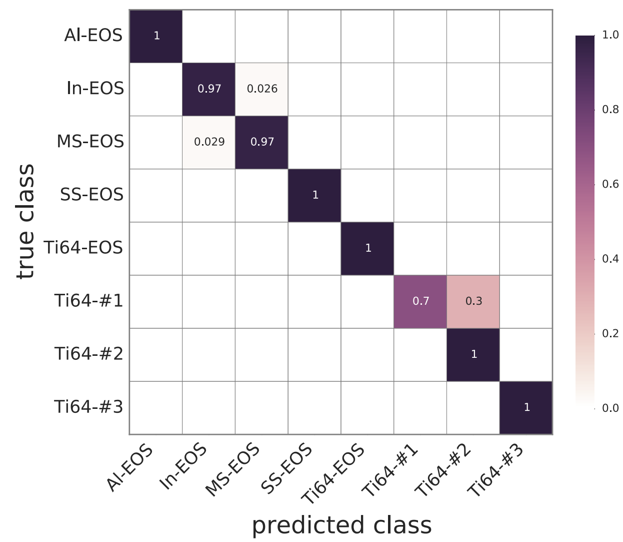

Bottom line: a computer can be trained to recognize and classify different types of powder far more reliably than any human, based on micrographs containing many particles.

Note: anomalous microstructures are also readily identified via similar techniques.

DeCost *et al.* (2017) *JOM* **69** 456

Carnegie Mellon University

Image Recognition Pipeline

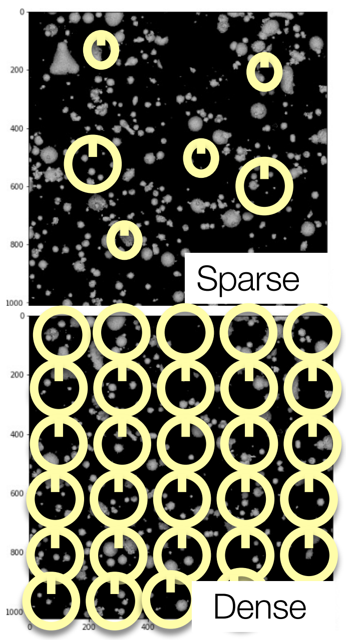

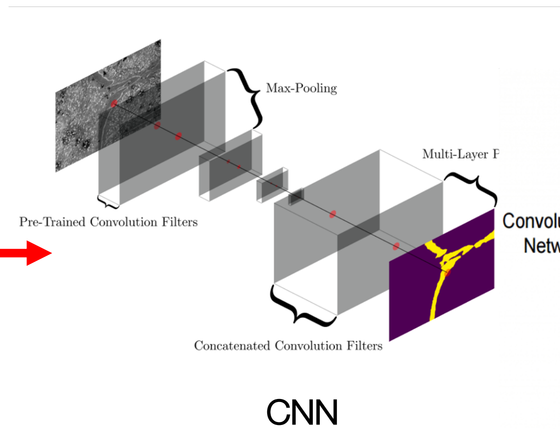

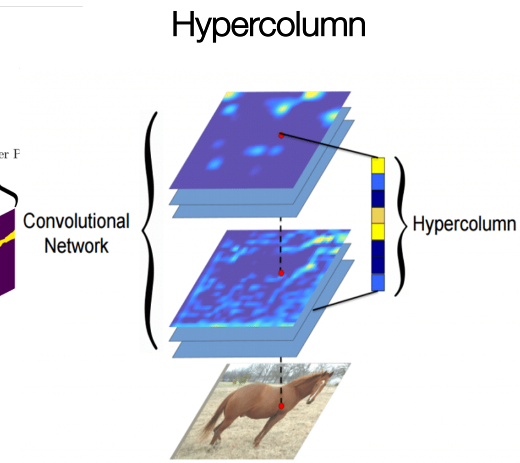

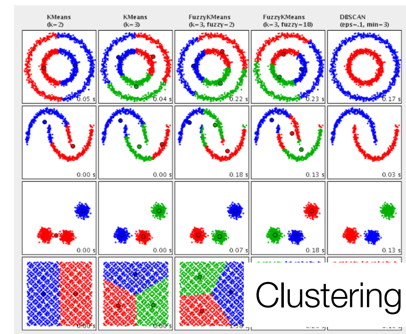

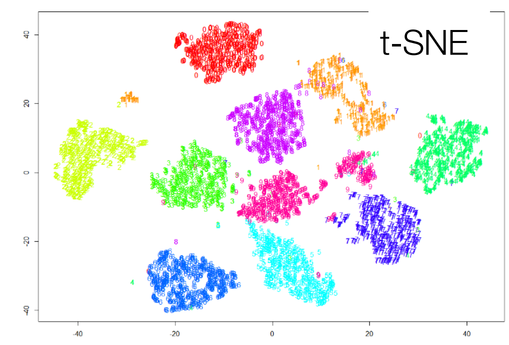

Image Feature Selection → Deep Learning Feature Extraction → Clustering → Visualization

Carnegie Mellon University

Steel Powder Feedstock

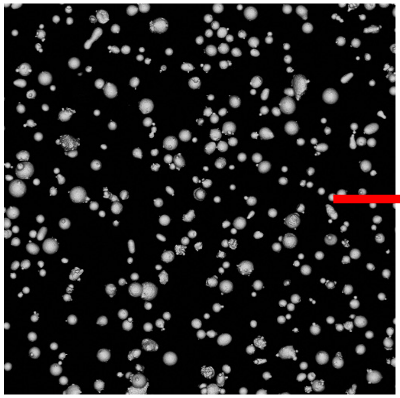

SEM Image

Steel Powder Feedstock

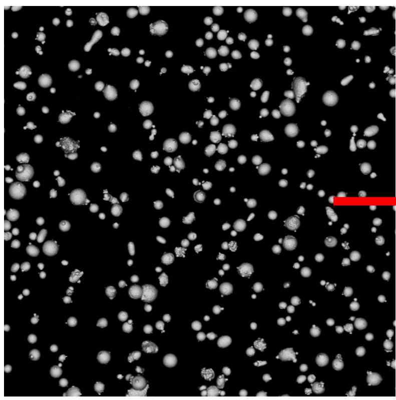

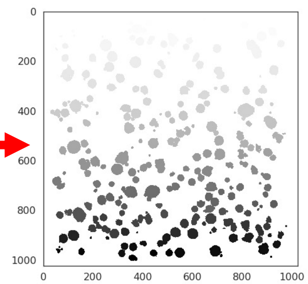

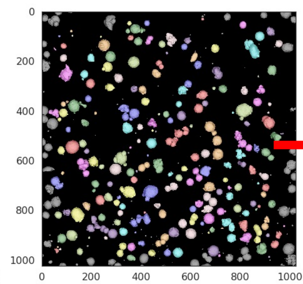

SEM Image

Segmented & Labelled Particles

Steel Powder Feedstock

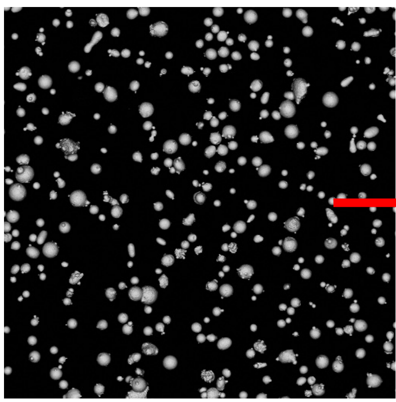

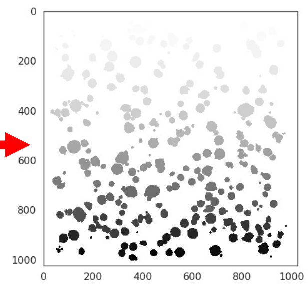

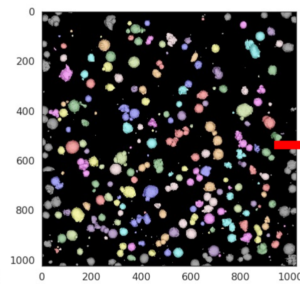

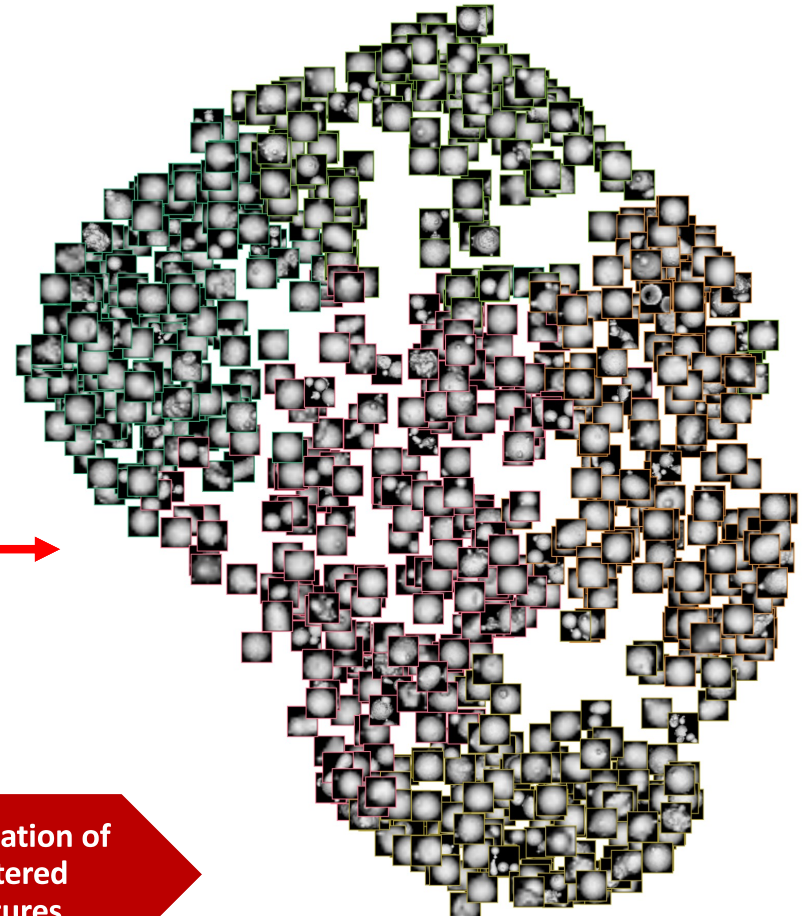

SEM Image

Segmented & Labelled Particles

Visualization of Clustered Features

Carnegie Mellon University

Steel Powder Feedstock: Classes of Powder Particles

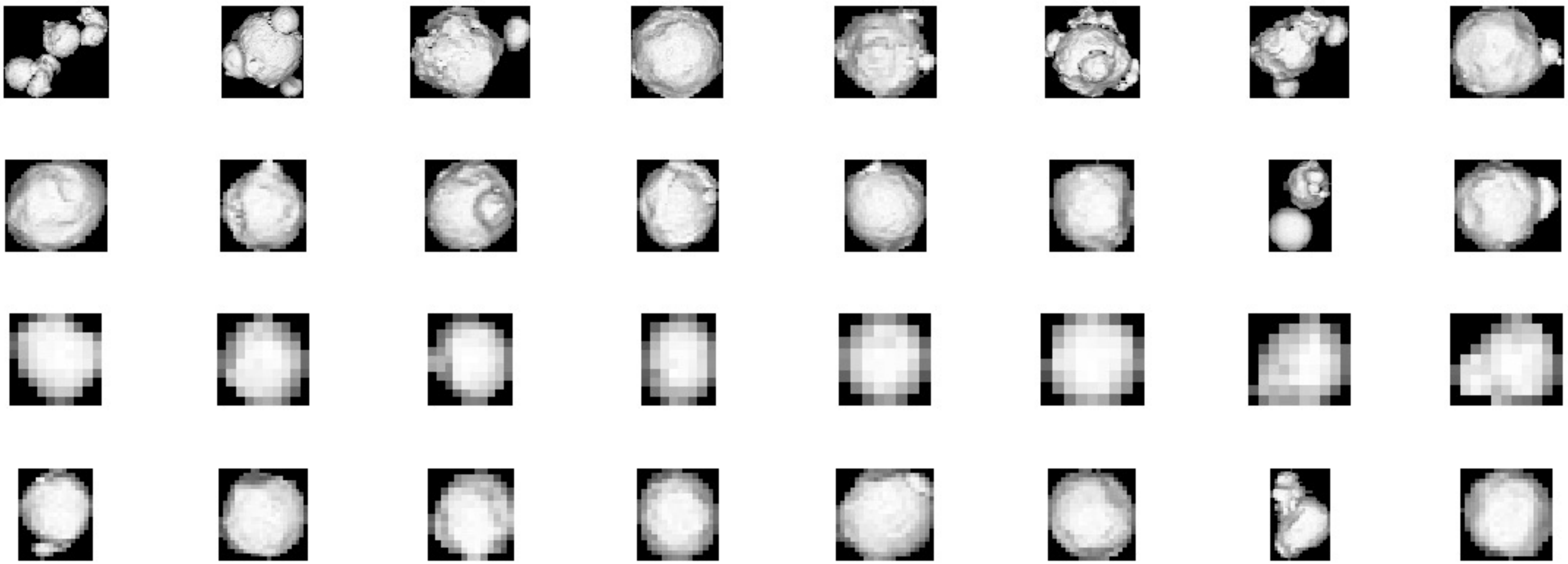

Recap

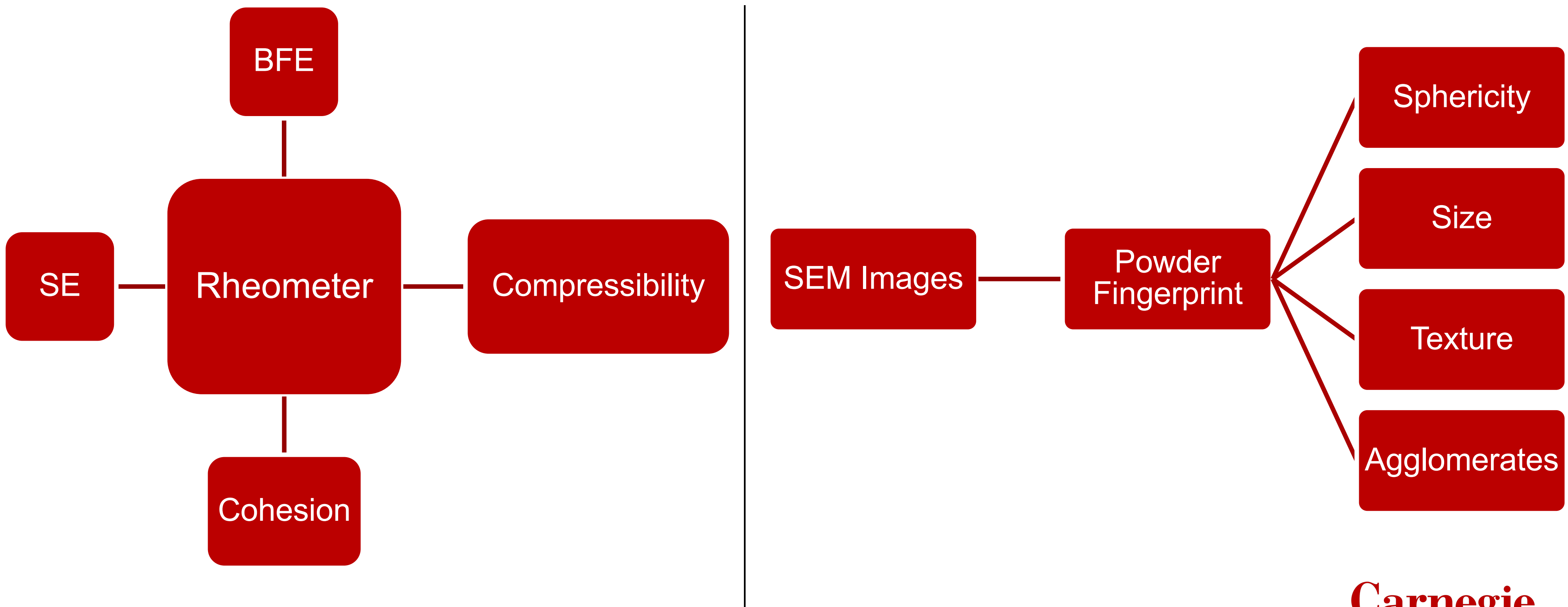

Carnegie Mellon University

Results: Flowability

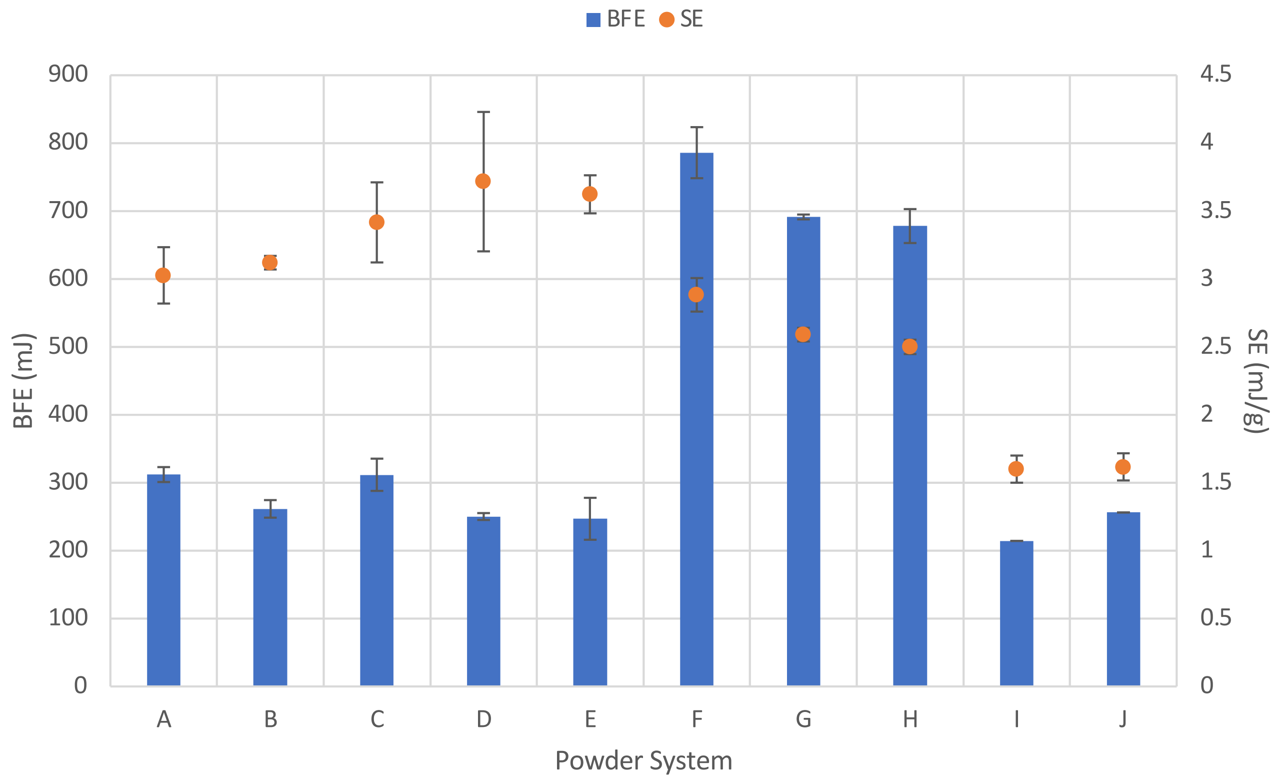

Definitions:
The Specific Energy, SE, is a measure of how powder will flow in an unconfined or low stress environment.
The Basic Flowability Energy, BFE, is the energy required to establish a particular flow pattern in a conditioned, precise volume of powder.

A: Proprietary Al Alloy
B: Proprietary Al Alloy
C: Proprietary Al Alloy
D: Proprietary Al Alloy
E: Proprietary Al Alloy
F: IN 718 GA
G: IN 718 Spheroidized
H: G after sieving
I: Ti64 HDH
J: Ti64 Standard GA

Having a low BFE coupled with a low SE usually indicates good flow properties. Exceptions occur if the BFE value is low but the SE value is high, that indicates that it may be either highly cohesive or have a large number of fines.

Carnegie Mellon University

Results: Flowability

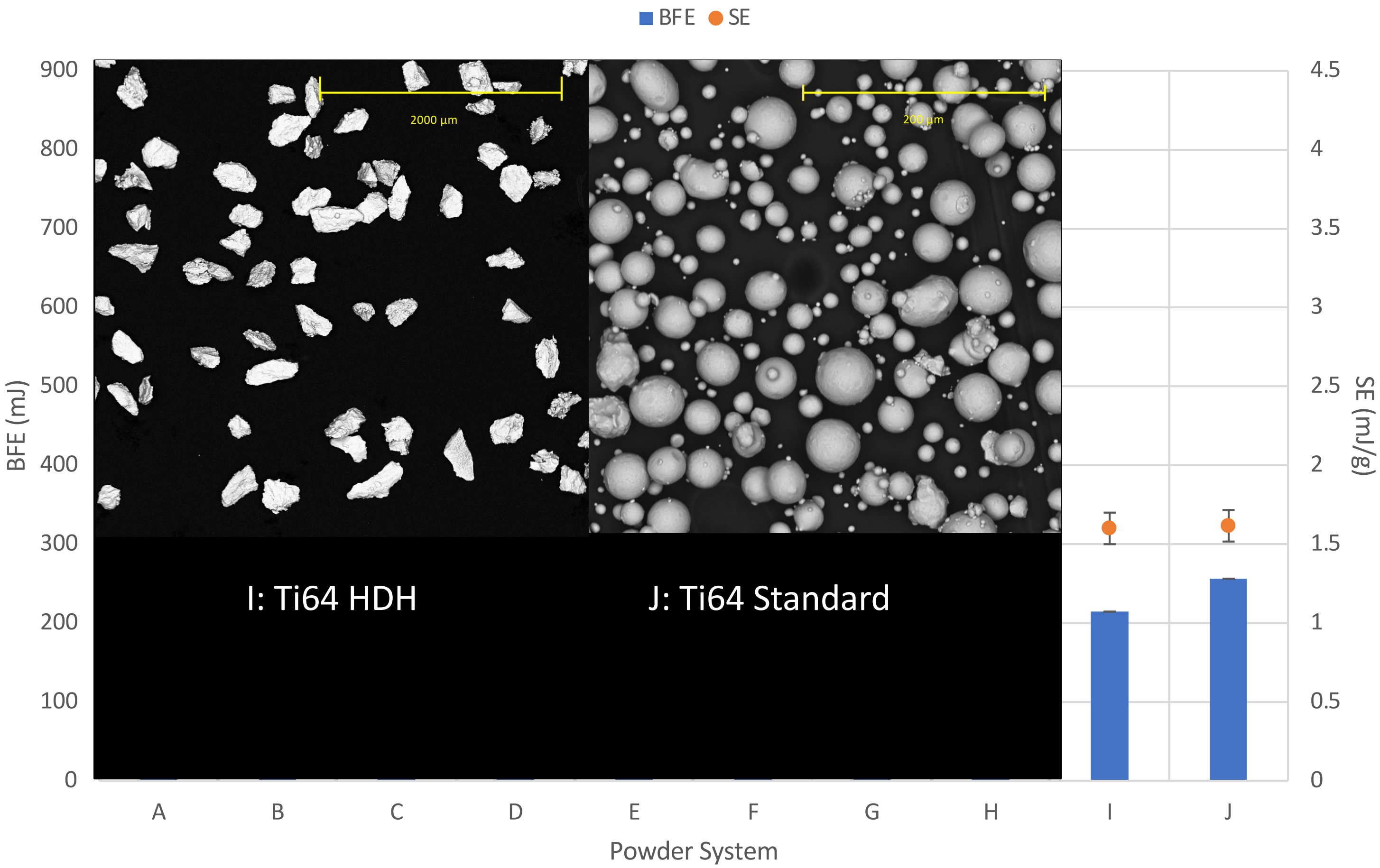

Surprising result: very different powder morphologies yield similar flow

Carnegie Mellon University

Results: Flowability

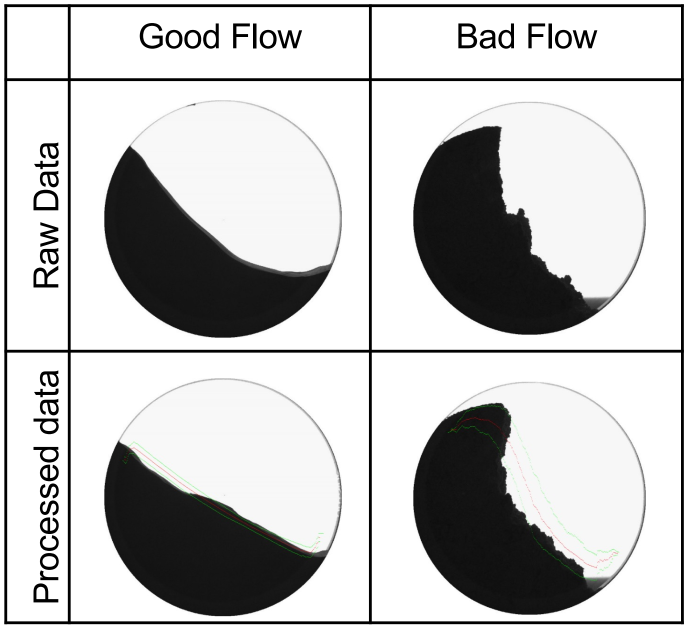

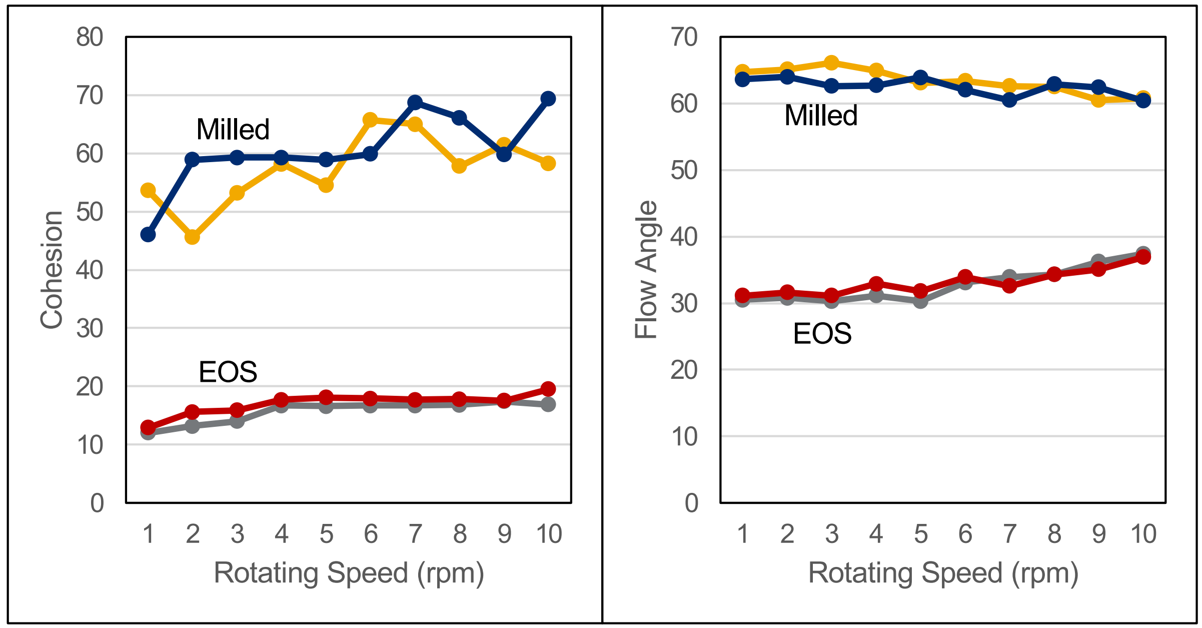

Two widely different performing powders were used to test the Granudrum with respect to its accuracy in characterizing flowability properties, with reasonable success.

Carnegie Mellon University

Results: Flowability

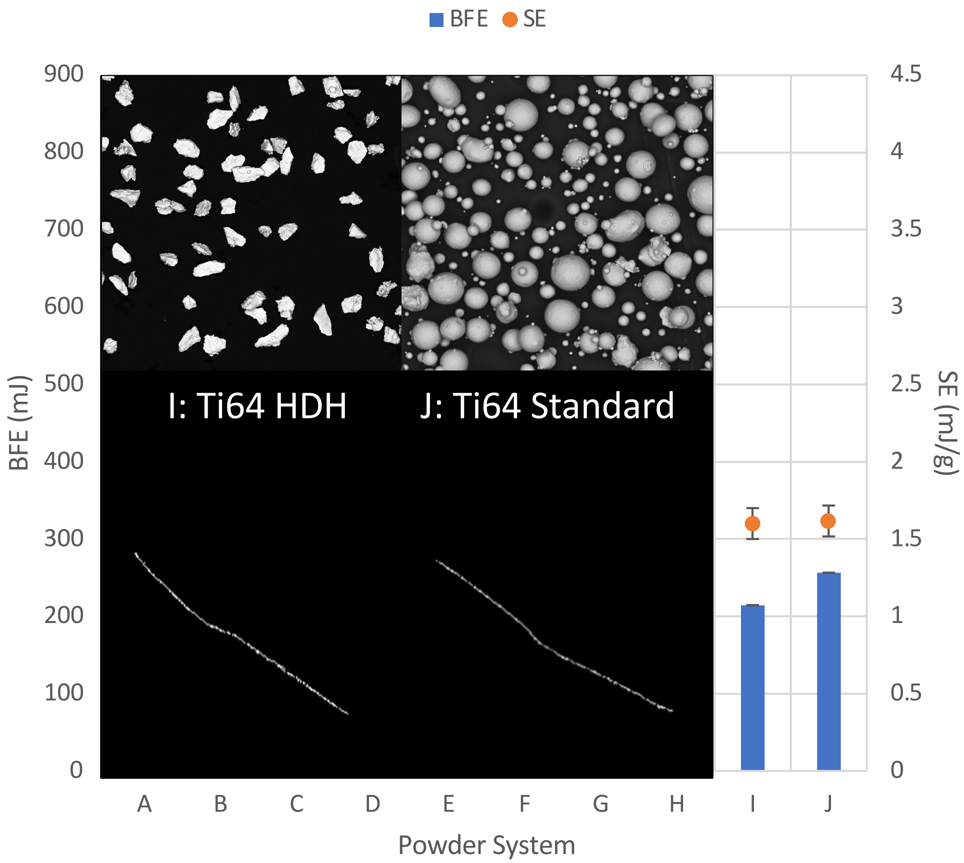

Consistency across flowability measurement systems: Granudrum vs FT4 Rheometer

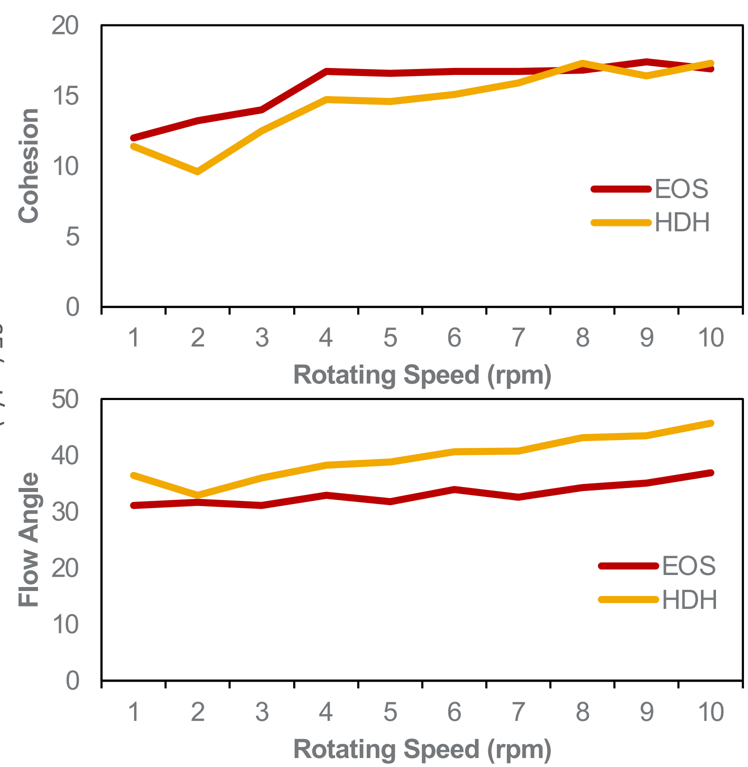

Carnegie Mellon University

Results: Flowability

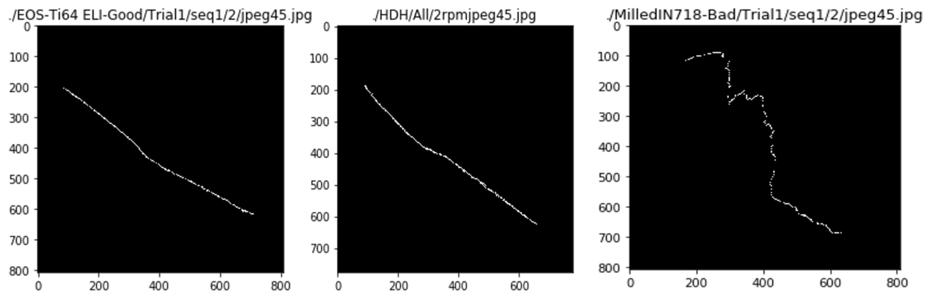

Powder Interfaces for Standard EOS Ti64, HDH Ti64, Milled IN718

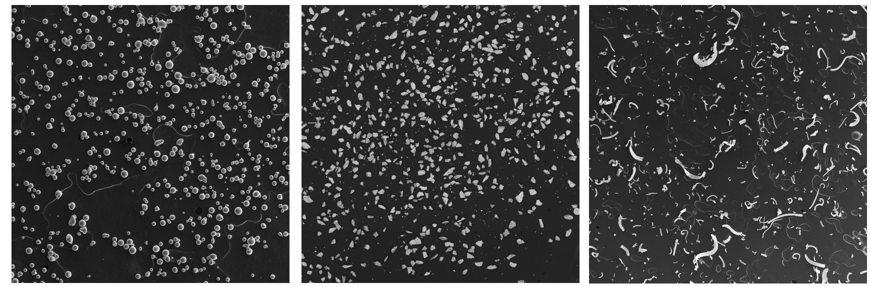
SEM Images for Standard EOS Ti64, HDH Ti64, Milled IN718 (50x)

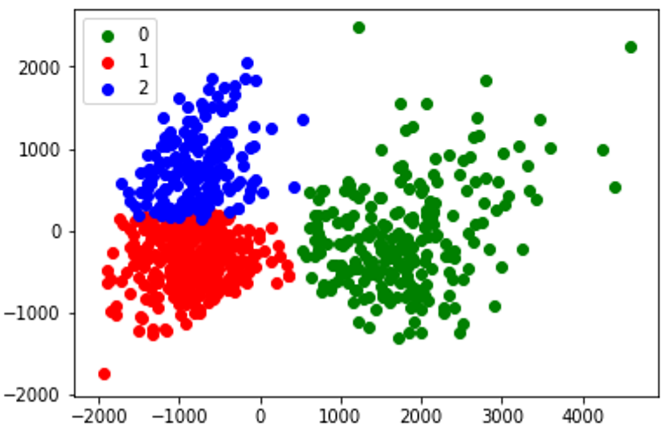

Powder Clusters according to Flowability

	0	1	2
0	0.96	0.02	0.008
1	0	0.53	0.47
2	0	0.24	0.76

Confusion Matrix

Milled IN718

EOS

HDH

Powder Interfaces were used to determine dynamic angle of repose that fit the interface with an R^2 of 0.98. This was used to cluster the powders according to their flowability. Each point represents one experiment run (with a particular speed).

The misclassification between EOS and HDH can be explained by looking at their dynamic flow angles which are quite similar for a slower rpm (e.g., 2) and differ significantly for higher rpm (e.g., 12)

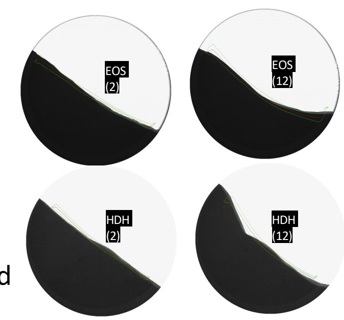

Carnegie Mellon University

Results: Flowability

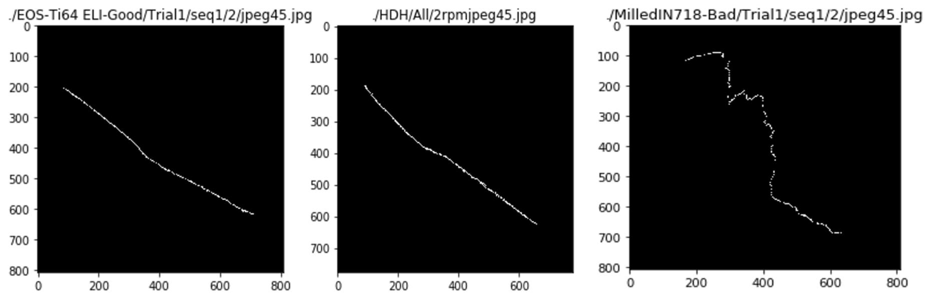

Powder Interfaces for Standard EOS Ti64, HDH Ti64, Milled IN718

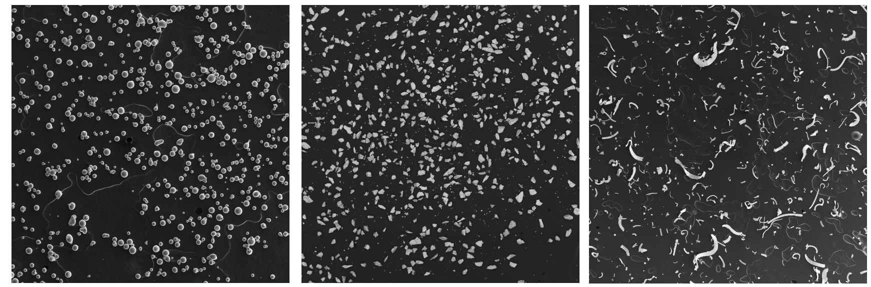
SEM Images for Standard EOS Ti64, HDH Ti64, Milled IN718 (50x)

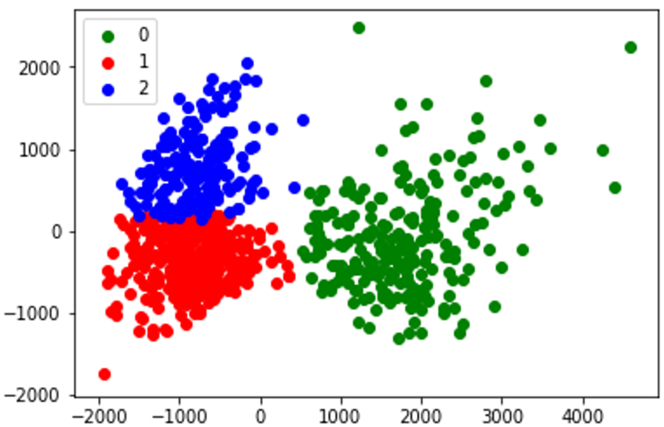

Powder Clusters according to Flowability

	0	1	2
0	0.96	0.02	0.008
1	0	0.53	0.47
2	0	0.24	0.76

Confusion Matrix

Milled IN718

EOS

HDH

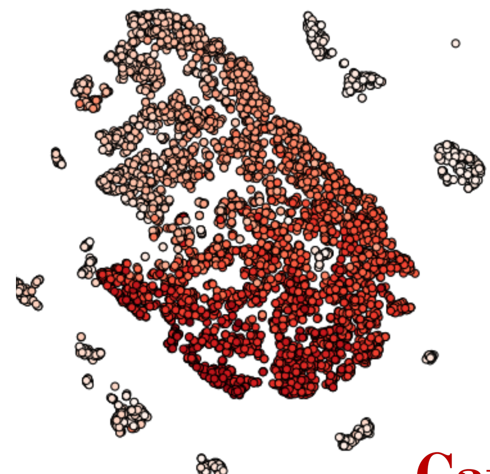
t-SNE plot of powder particles from three systems

Carnegie Mellon University

Potential to Answer AM Questions with Data Science

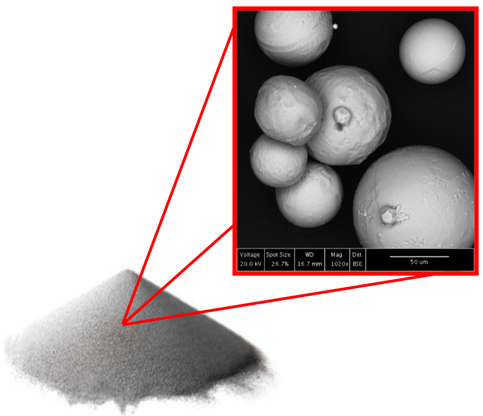

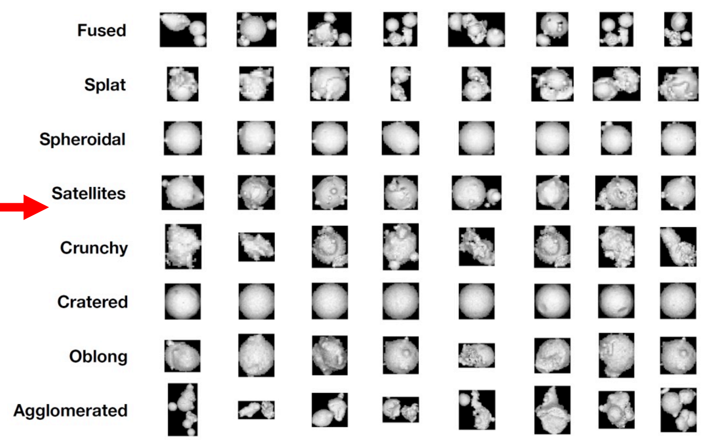

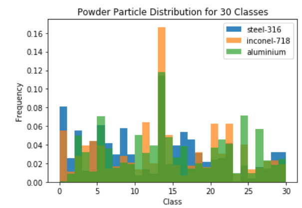

Quantitatively compare powders

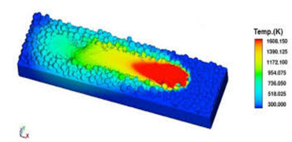

Develop flow coefficients for realistic powder based simulations

Establish cutoff point for the usage of recycled powder lots

It is possible to identify classes of similar particle morphology using CNNs and K-means clustering and t-SNE to visualize the data and then correlate to flow properties

Carnegie Mellon University

Acknowledgments

CMU Manufacturing Futures Initiative, supported by the W. K. Mellon Foundation.

Thank You!